Energy Budget and High-Gain Strategies for Voltage-Constrained Electrostatic Harvesters

Erick O. Torres, *Graduate Student Member, IEEE*, and Gabriel A. Rincón-Mora, *Senior Member, IEEE*
Georgia Tech Analog, Power, & Energy IC Research Lab
Email: ertorres@ece.gatech.edu, rincon-mora@ece.gatech.edu

***Abstract*—Wireless micro-sensors and similar technologies must derive their energy from micro-scale sources (e.g., thin-film Li Ions, etc.) to function in volume-constrained environments like the human body. Unfortunately, confining the source to small spaces limits the total energy available to such an extent that operational life is often impractically short. Ambient energy offers an alternate and virtually boundless source, except small volumes restrain harvesting power. Voltage-constrained electrostatic CMOS harvesters, for example, draw energy from the work done against the mechanical plates of a MEMS variable capacitor at relatively slow rates, producing low output power. This paper discusses how much energy is available in such a system before and after harvesting and offers energy-conservation schemes for increasing its net energy gain (i.e., power output) during all operational phases.**

I. Electrostatic Energy Harvesting

Electronic micro-devices like wireless micro-sensors [1]-[2] and biomedical implants [3] must often sense and transmit information noninvasively from difficult-to-reach and volume-constrained settings where recharging on-board miniaturized fuel cells and thin-film Li Ions are impractical luxuries [4]. Harvesting ambient energy, however, offers an alternate boundless source that promises to replenish continuously what the system consumes [5]. Kinetic energy in vibrations, for instance, is abundant in many environments and applications and can be harnessed from the work done against the electrostatic force in a micro-electromechanical systems (MEMS) variable capacitor [6]-[8]. Unlike their piezoelectric [9] and electromagnetic [10] counterparts, which require exotic materials, electrostatic harvesting is CMOS compatible because the source is a MEMS capacitor [7].

Allowing vibrations to decrease the capacitance of a variable capacitor (C_{VAR}) while keeping its voltage v_C or charge q_C constant produces energy in the form of charge or voltage, respectively ($q_C = C_{VAR}v_C$). Constraining q_C, however, generates unacceptably high voltages (e.g., $v_C \geq 250$ V) that normally exceed the breakdown limits of standard IC process technologies (e.g., ≤ 5-12 V) [11]. Clamping v_C, on the other hand, with the battery (V_{BAT}) to be charged, while allowing C_{VAR} to change, not only conveniently uses an already existing source but also limits v_C to V_{BAT}, driving harvested current directly to the battery [12].

Operationally, q_C flows out of C_{VAR} only when C_{VAR} decreases. This characteristic implies C_{VAR} must be clamped (i.e., pre-charged) to V_{BAT} at its maximum capacitance point ($C_{VAR(max)}$), just before C_{VAR} decreases and drives harvesting current i_{HARV} into the battery. As a result, drawing energy from C_{VAR} in response to vibrations requires a pre-charge phase at $C_{VAR(max)}$ (Fig. 1). After the harvesting phase that ensues, when C_{VAR} reaches its minimum point ($C_{VAR(min)}$), vibrations must again increase C_{VAR} to $C_{VAR(max)}$, which amounts to a reset phase.

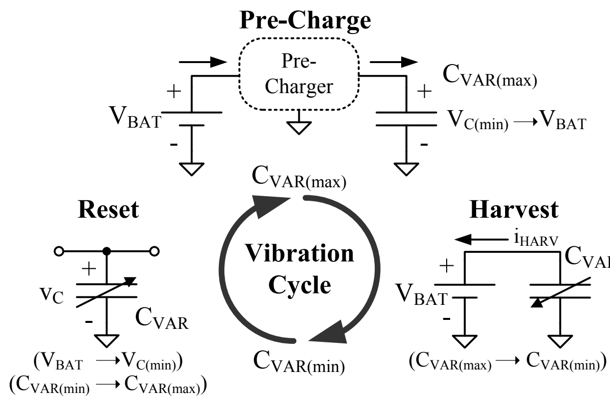

Fig. 1. Vibration cycle in an electrostatic energy harvester.

II. Energy Budget

To separate C_{VAR}'s plates, mechanical (vibration) force $F_{Mechanical}$ (Fig. 2) must exceed damping frictional and potential forces $F_{Friction}$ and $F_{Potential}$. The electrostatic force (F_E) that results in C_{VAR} is then proportional to the initial charge (as defined by pre-charge voltage V_{BAT}):

$$F_E(x) = \frac{Q^2}{2\varepsilon_o A} = \frac{\varepsilon_o A V_{BAT}^2}{2x^2}, \qquad (1)$$

where A is the total plate area, ε_o is the free space dielectric permittivity (8.85 pF/m), and x is the parallel-plate separation. As a result, the work (W) required to overcome F_E, or equivalently, the energy converted (E_{CONV}) after one vibration cycle depends on F_E and the resulting plate displacement (i.e., $x_{(max)} - x_{(min)}$), the latter of which translates to capacitance variation ΔC_{VAR}:

$$W = E_{CONV} = \int_{x_{(min)}}^{x_{(max)}} F_E(x)dx = \tfrac{1}{2}\Delta C_{VAR} V_{BAT}^2. \qquad (2)$$

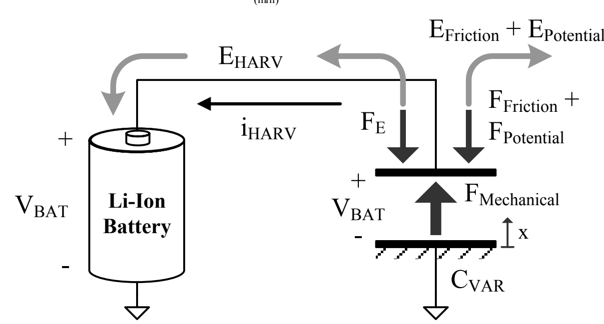

Fig. 2. Harvesting energy from a parallel-plate variable capacitor as vibrations separate its plates.

Note that pre-charging C_{VAR} at $C_{VAR(max)}$ to V_{BAT} represents an energy investment (E_{INV}) from the battery:

The authors thank Texas Instruments for supporting and sponsoring this research.

$$E_{INV} = \tfrac{1}{2} C_{VAR(max)} V_{BAT}^2 . \quad (3)$$

As C_{VAR} decreases, because v_C is kept at V_{BAT}, charge drifts out of C_{VAR} and into the battery, producing harvesting current source i_{HARV} or

$$i_{HARV} = \frac{dq_C}{dt} = \frac{d(C_{VAR} V_{BAT})}{dt} = V_{BAT}\left(\frac{dC_{VAR}}{dt}\right) \quad (4)$$

and a harvested energy gain per cycle (E_{HARV}) equivalent to

$$E_{HARV} = \int V_{BAT} i_{HARV}(t) dt = \Delta C_{VAR} V_{BAT}^2 . \quad (5)$$

Because C_{VAR} remains at V_{BAT} when it reaches $C_{VAR(min)}$, it retains remnant energy E_{REM} after the harvesting phase:

$$E_{REM} = \tfrac{1}{2} C_{VAR(min)} V_{BAT}^2 . \quad (6)$$

Recovering E_{REM} after harvesting E_{HARV}, considering the battery lost E_{INV}, generates a net theoretical energy gain per cycle (E_{NET}) in the battery of

$$E_{NET} = -E_{INV} + E_{HARV} + E_{REM} = \tfrac{1}{2} \Delta C_{VAR} V_{BAT}^2 , \quad (7)$$

which is the energy harnessed from the environment (Eq. 2).

Considering E_{REM} is substantially low and comparable to the losses associated with transferring it, attempting to recover it offers little to no gain. It is therefore often times more efficient to lose E_{REM} by keeping C_{VAR} open-circuited when its plates pull together. Still, a net energy gain per cycle remains after losing E_{REM}:

$$E_{NET} = -E_{INV} + E_{HARV} = \left(\tfrac{1}{2} C_{VAR(max)} - C_{VAR(min)}\right) V_{BAT}^2 . \quad (8)$$

Nevertheless, even if energy in the environment is virtually boundless, only small packets can be drawn at a time, which means power is low. The problem is that the bias, control, and power circuit pre-charging C_{VAR} and transferring energy from C_{VAR} to the battery require energy, possibly reducing E_{NET} to impractical levels, which is why high efficiency in all phases of operation is so important.

III. PRE-CHARGE PHASE

When considering energy-transfer strategies, pre-charging C_{VAR} to V_{BAT} with a switch (Fig. 3) incurs a fundamental power loss not present in inductor-based circuits because the voltage across the former does not exist in the latter. Charging $C_{VAR(max)}$ from zero to V_{BAT} with a switch, for instance, irrespective of its resistance R, requires a switch energy E_{Switch} that is equal to the initial investment needed in C_{VAR}:

$$E_{Switch} = \int_0^\infty v_R(t) i_R(t) dt = \tfrac{1}{2} C_{VAR(max)} V_{BAT}^2 = E_{INV} . \quad (9)$$

In other words, the battery loses $2E_{INV}$ to invest E_{INV} in C_{VAR} (i.e., 50% efficiency).

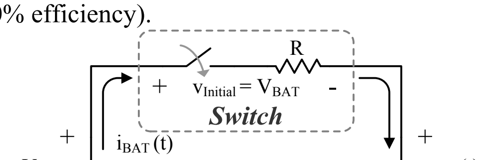

Fig. 3. Pre-charging C_{VAR} with a switch.

No energy is lost (in theory), however, when channeling investment energy E_{INV} to C_{VAR} via a transfer inductor (L_X), as shown in Fig. 4. The reason for this lossless transaction is that energizing L_X from V_{BAT} via switch S_P does not expose S_P to a voltage because, while L_X's current rises (L_X energizes), L_X's switching terminal voltage v_{SW} remains within mV's of V_{BAT} through the entire energizing period. Similarly, de-energizing L_X into C_{VAR} keeps the voltage across switch S_N close to zero because, while L_X's current falls (L_X de-energizes), v_{SW} remains within mV's of ground. Note the pre-charger disengages during the harvesting phase so S_P and S_N shut off after the pre-charge phase terminates, analogous to a switching converter under discontinuous conduction conditions.

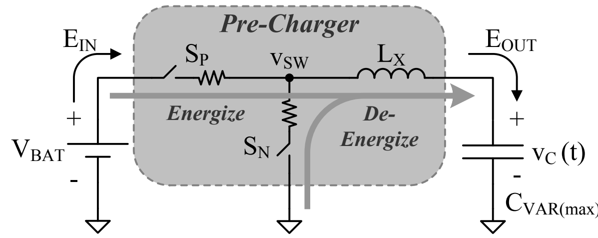

Fig. 4. Magnetic-based (inductor-based) pre-charger circuit.

Key to the success of this circuit is to deliver no more *and* no less than E_{INV}, and do so with minimal control circuits. To this end, consider that during the energizing period, both L_X and C_{VAR} energize with a total LC energy (E_{LC}) of

$$E_{LC}(t) = C_{VAR(max)} V_{BAT}^2 \left[1 - \cos(\omega_{LC} t)\right], \quad (10)$$

as derived in the Appendix, where ω_{LC} is LC's resonant frequency. As a result, E_{LC} reaches E_{INV} in one-sixth ω_{LC}'s equivalent period, which corresponds to a C_{VAR} target voltage of $0.5V_{BAT}$. In other words, S_P should engage and allow the battery to energize L_X and C_{VAR} until C_{VAR} charges to $0.5V_{BAT}$, after which point S_N should allow L_X to finish charging C_{VAR} to its target of V_{BAT}.

Note that although the energy invested by the battery (E_{INV}) equals the energy received in C_{VAR}, the total charge lost by the battery does not equal the charge gained in C_{VAR}. This difference arises because of the voltage inequality between the two, as drawing power from a larger voltage (e.g., V_{BAT} is less than $V_{C(Initial)}$) requires less current. The total charge collected in C_{VAR} ($\Delta q_{C(pre)}$) as it charges from zero, for instance, is

$$\Delta q_{C(pre)} = C_{VAR(max)} V_{BAT} , \quad (11)$$

whereas the charge lost by the battery ($\Delta q_{BAT(pre)}$) is

$$\Delta q_{BAT(pre)} = \int_{\Delta t_E} i_{BAT}(t) dt = \tfrac{1}{2} C_{VAR(max)} V_{BAT} , \quad (12)$$

which is half the final charge in C_{VAR}.

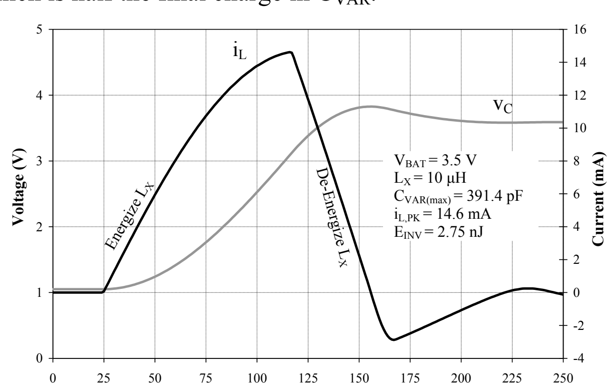

Fig. 5. L_X current and C_{VAR} voltage waveforms during the pre-charge phase.

In practice, the magnetic-based pre-charge circuit is not completely free of energy losses [12]. For instance, the voltages across the switches are small but not zero, inducing finite conduction losses, and parasitic capacitors present require energy to charge and discharge. In the simulations results shown in Fig. 5, for example, a 3.5 V battery invests 2.75 nJ (with a peak current of 14.6 mA through 10 μH) to pre-charge 391.4 pF from 1.05 V (which had 0.22 nJ stored from the previous reset phase). What is perhaps more troubling is the control circuitry used to monitor and drive the switches because they demand power to operate. Fortunately, all these power losses occur during a small fraction of the entire vibration cycle so the total energy lost is substantially low. Operating the control circuit for 125 ns (Fig. 5) at 50 μA from the 3.5 V battery would only require 22 pJ, which amounts to a negligibly small fraction of the total investment.

Nevertheless, to charge C_{VAR} fully in the presence of losses, the battery must over-invest energy. Doing so amounts to increasing the energizing target voltage (and related energizing time t_E) from $0.5V_{BAT}$ to a higher value (e.g., $0.8V_{BAT}$ in Fig. 5). Circuit conditions and temperature change over time, however, shifting the ideal target in the process. A slow feedback loop that senses excess energy in C_{VAR} over several cycles and modulates the energizing target voltage corrects for the effects of changing conditions across time. For instance, comparing C_{VAR}'s voltage after the pre-charge phase ($V_{C(Final)}$) against V_{BAT} dictates whether t_E should be incrementally increased or decreased (e.g., increase t_E if $V_{C(Final)} < V_{BAT}$). In steady state, t_E converges to its optimal value, ensuring C_{VAR} pre-charges to V_{BAT}, regardless of losses across the circuit and the actual value of $C_{VAR(max)}$.

IV. Harvesting Phase

When harvesting via a switch (Fig. 6(a)), vibrations separate C_{VAR}'s parallel plates (i.e., C_{VAR} decreases) and drives charge q_{HARV} (i.e., i_{HARV}) and energy $E_{C(HARV)}$ into the battery:

$$q_{HARV} = \Delta C_{VAR} V_{BAT} \quad (13)$$

and

$$E_{C(HARV)} = \tfrac{1}{2}\Delta q_{HARV} V_{BAT} = \tfrac{1}{2}\Delta C_{VAR} V_{BAT}^2. \quad (14))$$

Note this energy is half the total energy received by the battery (E_{HARV} or $\Delta C_{VAR} V_{BAT}^2$, as derived earlier). The difference represents the mechanical input to the system, that is, the battery's ideal net energy gain (E_{NET}), as previously derived.

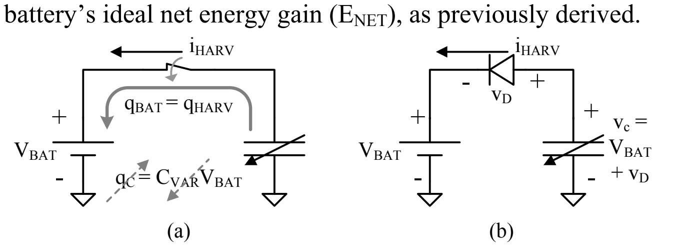

Fig. 6. Harvesting current via (a) an ideal switch or (b) a diode.

The simplest embodiment of the switch is an asynchronous diode because no circuit (i.e., power) is required to control it, as it automatically conducts the harvesting current to the battery when available and blocks reverse current when C_{VAR} reaches $C_{VAR(min)}$. The drawback is its forward voltage drop (v_D), which implies no current flows until v_C rises from pre-charged voltage $V_{C(Final)}$ to $V_{BAT} + v_D$ and corresponds to C_{VAR} decreasing from $C_{VAR(max)}$ to $C_{VAR(max)}$' under charge-constrained conditions. In other words, the total capacitance variation reduces from ΔC_{VAR} to ΔC_{VAR}' or

$$\Delta C_{VAR}' = \left(\frac{V_{C(Final)}}{V_{BAT} + v_D}\right) C_{VAR(max)} - C_{VAR(min)}, \quad (15)$$

which implies some of the converted energy (E_{HARV}) is diverted from the battery to overcome v_D. This remains true even when considering a higher v_C induces a higher harvesting current (i_{HARV}') because harvesting time t_{HARV}' is now shorter by the length of time C_{VAR} takes to reach $C_{VAR(max)}$':

$$i_{HARV}' = \frac{q_{HARV}'}{t_{HARV}'} = \frac{(V_{BAT} + v_D)\Delta C_{VAR}'}{t_{HARV}'}. \quad (16)$$

As a result, v_D reduces harvested energy gain (E_{HARV}') to

$$E_{HARV}' = q_{HARV}' V_{BAT} = \left[(V_{BAT} + v_D)\Delta C_{VAR}'\right] V_{BAT}. \quad (17)$$

Pre-charging C_{VAR} to $V_{BAT} + v_D$ circumvents the brief charge-constrained event mentioned and recovers the full C_{VAR} variation, but requires a higher energy investment E_{INV}' from the battery. The problem is the optimum pre-charge voltage ($V_{C(Final)}$) of the system is V_{BAT} so $V_{BAT} + v_D$ produces a less-than-optimal net energy gain per cycle E_{NET}'. For proof, consider that differentiating E_{NET} or

$$E_{NET}' = E_{HARV}' - E_{INV} = E_{HARV}' - \tfrac{1}{2} C_{VAR(max)} V_{C(Final)}^2 \quad (18)$$

with respect to $V_{C(Final)}$, equating to zero, and solving for $V_{C(Final)}$ yields V_{BAT}. A diode therefore produces a non-optimal net energy gain of

$$E_{NET}' = E_{NET} - C_{VAR(min)} v_D V_{BAT}, \quad (19)$$

which compared to an ideal switch case (Eq. 8), yields lower energy, as shown in Fig. 7 where a 400-100 pF C_{VAR} variation harvests 3.45 nJ and 3.69 nJ with and without the diode, respectively. The 0.7 V drop decreased $C_{VAR(max)}$ from 400 pF to about 330 pF, reducing energy by 240 pJ per cycle (by 6.5%), which is significant considering how difficult decreasing losses at these low power levels is.

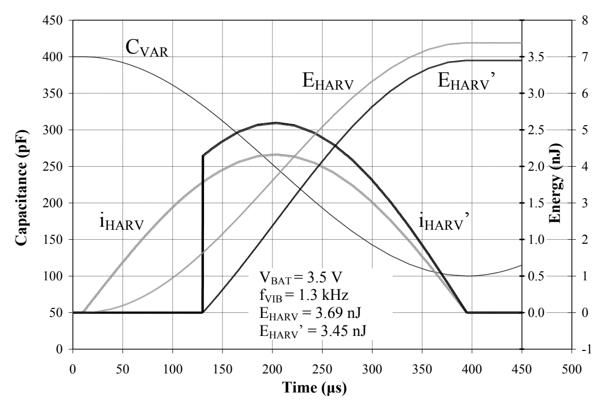

Fig. 7. Currents and harvested energy in switch- and diode-based circuits.

A synchronous transistor switch, with respect to its voltage drop, more closely resembles an ideal switch, except it requires a circuit (i.e., power) to control it and drive the parasitic capacitors it presents. The two back-to-back PMOS transistors shown in Fig. 8, for example, constitute a sample embodiment of the synchronous switch, where each device blocks the other's body diode from conducting when disengaged [12]. Using the synchronous switch merits scrutiny and possible adoption, but only if the control circuit uses sufficiently less energy than what the diode effectively loses, which is why biasing circuits in sub-threshold is important.

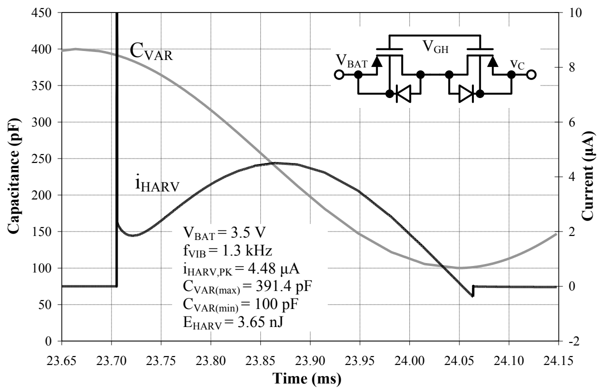

Fig. 8. Energy harvesting with a PMOS-based switch.

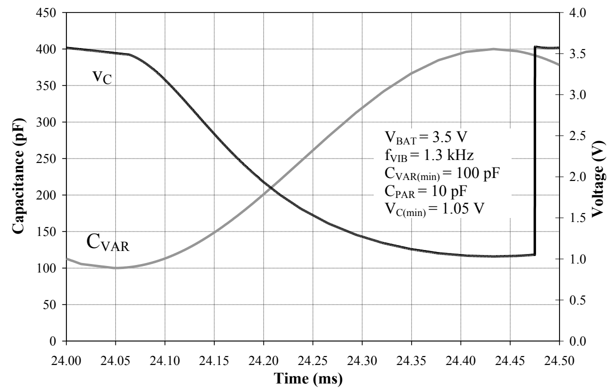

Fig. 9. Capacitor voltage as C_{VAR} increases during reset phase.

V. Reset Phase

As mentioned earlier, remnant energy E_{REM} in C_{VAR} after the harvesting phase is not large enough (pJ's) to warrant recovering it. Simply disengaging the harvesting switch (while still disconnected from the pre-charge circuit) leaves C_{VAR} open-circuited during the reset phase, when it increases from $C_{VAR(min)}$ to $C_{VAR(max)}$. Increasing C_{VAR} under these charge-constrained conditions has the effect of decreasing v_C to a fraction of V_{BAT}:

$$V_{C(min)} = \left(\frac{C_{VAR(min)}}{C_{VAR(max)}}\right)V_{BAT}, \tag{20}$$

as the simulation results of Fig. 9 shows. In essence, C_{VAR}'s electrostatic force F_E now helps vibrations pull the plates together, converting some of its remnant energy E_{REM} back to the mechanical domain.

Even though this E_{REM} does not return to the battery, it can be nonetheless used and not really lost. The fact is changes in v_C indicate the state of C_{VAR}, and detecting when C_{VAR} reaches $C_{VAR(max)}$ is required to start the subsequent pre-charge phase. In other words, E_{REM} is used by the control circuit, diminishing its negative impact on the system's net energy gain per cycle. Not taking advantage of this effect increases the complexity and power requirements of the control circuit by requiring a capacitance-sensing block.

VI. Conclusion

Increasing the energy gain of an electrostatic voltage-constrained energy harvester amounts to understanding its energy budget and reducing the losses associated with each operational phase. Using an inductor-based pre-charger, for example, increases the pre-charger efficiency from 50% to 79%; using a transistor switch as the harvesting medium (instead of a diode) saves 240 pJ/cycle; and using the remnant energy left in C_{VAR} after the harvesting phase to sense its capacitance reduces circuit complexity and control power. Operating the control circuit in sub-threshold and regulating the pre-charge target voltage to V_{BAT} (its optimal target) over the span of several cycles (with a slow feedback loop) further optimize the system and increase its energy gain per cycle (i.e., output power). Extracting more energy from vibrations means micro-scale systems such as wireless micro-sensors and biomedical implants can replenish more of the power they consume, extending operational life in the process.

Appendix

While energizing, the pre-charge circuit (Fig. 4) can be described as a differential equation, which, assuming both i_L and v_C are initially zero, results in the following:

$$v_C(t) = V_{BAT}\left(1 - \cos(\omega_{LC}t)\right), \tag{A.1}$$

$$i_L(t) = V_{BAT}\sqrt{\frac{C_{VAR(max)}}{L_X}}\sin(\omega_{LC}t), \tag{A.2}$$

where ω_{LC} is the LC's natural resonant frequency and equal to $1/\sqrt{(L_X C_{VAR(max)})}$. The battery energizes the LC circuit, where the stored energy in both components equals:

$$E_{LC}(t) = \tfrac{1}{2}L_X i_L^2(t) + \tfrac{1}{2}C_{VAR(max)}v_C^2(t), \tag{A.3}$$

and therefore:

$$E_{LC}(t) = C_{VAR(max)}V_{BAT}^2\left[1 - \cos(\omega_{LC}t)\right]. \tag{A.4}$$

References

[1] D. Puccinelli and M. Haenggi, "Wireless sensor networks: applications and challenges of ubiquitous sensing," *IEEE Circuits and Systems Magazine*, v. 3, n. 3, p. 19-29, 2005.

[2] J.P. Vogt and G.A. Rincón-Mora, "SiP wireless micro-power sensors," *Govt. Microcircuit Apps. and Critical Tech. Conf.*, Mar. 2007.

[3] P. Dario, et al., "Micro-systems in biomedical applications," *J. of Micromech. and Microeng.*, v. 10, n. 2, p. 235-244, June 2000.

[4] M. Chen, J.P. Vogt, and G.A. Rincón-Mora, "Design methodology of a hybrid micro-scale fuel cell-thin-film lithium ion source," *IEEE MWSCAS*, p. 674-677, Aug. 2007.

[5] E. Torres and G. Rincón-Mora, "Energy-harvesting system-in-package (SiP) microsystem," *ASCE J. of Energy Eng.*, v. 134, Dec. 2008.

[6] S.P. Beeby, M.J. Tudor, and N.M. White, "Energy harvesting vibration sources for microsystems applications," *Measurement Science and Technology*, v. 17, n. 12, p. R175-195, Dec. 2006.

[7] S. Roundy, P.K. Wright, and J.M. Rabaey, *Energy Scavenging for Wireless Sensor Networks with Special Focus on Vibrations*, 1st ed., Massachusetts: Kluwer Academic Publishers, 2004.

[8] P.D. Mitcheson, et al., "Architectures for vibration-driven micropower generators," *IEEE J. of MEMS*, v. 13, n. 3, p. 429-440, June 2004.

[9] E. Lefeuvre, et al., "Buck-boost converter for sensorless power optimization of piezoelectric energy harvester," *IEEE Trans. on Power Electronics*, v. 22, n. 5, p. 2018-2025, Sept. 2007.

[10] S.P. Beeby, et al., "A micro electromagnetic generator for vibration energy harvesting," *J. of Micromech. and Microeng.*, v. 17, p. 1257-1265, July 2007.

[11] B.H. Stark, et al., "Converter circuit design, semiconductor device selection and analysis of parasitics for micropower electrostatic generators," *IEEE Trans. on Power Electronics*, v. 21, n. 1, p. 27-37, Jan. 2006.

[12] E.O. Torres and G.A. Rincón-Mora, "Electrostatic energy harvester and Li-Ion charger for micro-scale applications," *IEEE MWSCAS*, p. 65-69, Aug. 2006.